JOURNAL OF THEORETICAL
AND APPLIED MECHANICS
46, 4, pp. 813-828, Warsaw 2008

OPTIMIZATION OF ELASTIC ANNULAR PLATES SUBJECT TO THERMAL LOADINGS WITH RESPECT TO VIBRATION

Antoni Gajewski

Cracow University of Technology, Institute of Physics, Kraków, Poland

e-mail: dantek@fizyk.ifpk.pk.edu.pl

In the paper, the optimization of annular plates subject to circularly symmetric distribution of thermal loading with respect to vibration frequency is considered. What is searched for is such a distribution of plate thickness of a constant volume which maximizes its lowest vibration frequency. The studies are confined to a plate clamped at the inner and outer edges and to one type of non-homogeneous temperature distribution. The inequality constraints on the minimal and maximal values of the plate thickness are taken into account. The applied method of solution is the Pontryagin maximum principle combined with sensitivity analysis and a gradient procedure.

Key words: optimization, annular plate, thermal loading

1. Introduction

The optimization of circular and annular plates compressed by uniformly distributed conservative loadings with respect to stability were considered in several papers, e.g. by Frauenthal (1972), Grinev and Filippov (1977), Rzegocińska-Pełech and Waszczyszyn (1984), Mermertas and Belek (1990), Wróblewski (1992). Some non-conservative problems of the optimization of circular plates were presented by Gajewski and Cupiał (1992) and Gajewski (2002a,b).

Recently, a formulation of the optimization problem of annular plates under thermal loadings with respect to buckling was presented by Gajewski (2001) who considered a non-uniform elastic annular plate subject to a non-uniformly distributed temperature field. Similar problems were analysed by Krużelecki and Smaś (2006) who obtained optimal solutions for different modes of supports and different ratios of inner and outer radii. The methods of moving asymptotes and simulated annealing were used. A more general problem of an annular plate optimization was formulated by Gajewski (2002b) who optimized the radially distributed thickness of a plate $h(x)$ with respect to vibration under a constant volume condition and constant temperature loading. To this end, the Pontryagin maximum principle with sensitivity analysis and an iterative procedure were used.

The principal aim of this paper is a broader presentation of some new results of numerical calculations obtained for a similar problem.

2. Formulation of the optimization problem

The principal aim of the present paper is to optimize the radially distributed thickness $\overline{h}(\overline{r})$ of a thin annular plate with respect to vibration (or buckling) under a constant volume condition. The plate supported in different ways is subject to thermal loading by an increment of temperature, which can be radially distributed in a specific way $\overline{T}(\overline{r})$ (Fig. 1). We look for such a thickness distribution so as to maximize the lowest frequency of vibration under a given constant thermal loading and a given volume of the plate. In particular, if the first frequency of vibration is equal to zero we can maximize the first critical thermal loading. Generally, the equations of the precritical and vibration states should be analysed. The constant volume condition will be written in a dimensionless form

$$\int_{\beta}^{1} xh(x)\,dx = 1 \tag{2.1}$$

where the dimensionless functions and parameters are defined by (4.3) and (4.5).

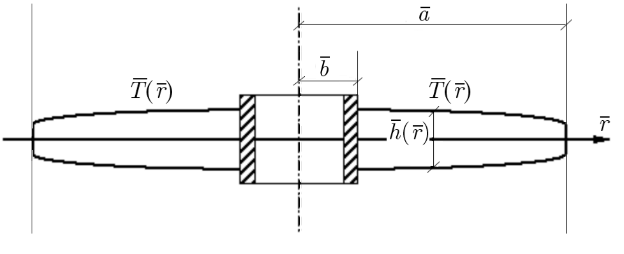

Fig. 1. An annular plate under thermal loading

3. The optimization methods

3.1. Pontryagin maximum principle

To solve the presented optimization problem, we use the Pontryagin maximum principle in its classical form, combined with a sensitivity analysis formulation. To this end, the membrane and vibration state equations with boundary conditions will be written in the forms (cf. Gajewski and Życzkowski, 1988):

$$
\begin{array}{lll}
Y_i' = G_i(x, Y_i, h, P) & i = 1, 2 & \\
\widetilde{\mu}_{1\gamma} Y_\gamma(\beta) = 0 & \widetilde{\nu}_{2\gamma} Y_\gamma(1) = 0 & \gamma = 1, 2
\end{array}
\tag{3.1}
$$

$$
\begin{array}{lll}
Z_i' = A_{i\alpha}(x, h, P, \omega) Z_\alpha & i = 1, \dots, 4 & \alpha = 1, \dots, 4 \\
\mu_{j\alpha} Z_\alpha(\beta) = 0 & \nu_{j\alpha} Z_\alpha(1) = 0 & j = 1, 2
\end{array}
\tag{3.2}
$$

where $Y_i(x)$ and $Z_i(x)$ denote membrane and vibration state variables, respectively, A_{ij} is a matrix dependent on the loading parameter and frequency of vibration, G_i are certain functions (in our case, the generally nonlinear functions G_i are linear with respect to Y_i) and $\widetilde{\mu}_{1\gamma}$, $\widetilde{\nu}_{2\gamma}$, $\mu_{j\alpha}$, $\nu_{j\alpha}$ are given matrices of constant parameters. In the paper, the summation convention is used. Therefore, the Hamiltonian and appropriate adjoint equations connected with the state equations and constant volume condition (2.1) are as follows

$$
H = \chi_\alpha G_\alpha + \psi_\beta A_{\beta\gamma} Z_\gamma + \Lambda x h \tag{3.3}
$$

$$
\chi_\alpha = -\frac{\partial H}{\partial Y_\alpha} \qquad\qquad \psi_\beta = -\frac{\partial H}{\partial Z_\beta} \tag{3.4}
$$

and $\alpha = 1, 2$, $\beta = 1, \dots, 4$, $\gamma = 1, \dots, 4$.

The optimal control function $h(x)$ should be determined from the supremum condition of the Hamiltonian

$$
M(\boldsymbol{\chi}, \boldsymbol{\psi}, \widetilde{\boldsymbol{Y}}, \widetilde{\boldsymbol{Z}}) = \sup_{h \in \widetilde{h}} H(h, \boldsymbol{\chi}, \boldsymbol{\psi}, \widetilde{\boldsymbol{Y}}, \widetilde{\boldsymbol{Z}}) \tag{3.5}
$$

3.2. Sensitivity analysis

Calculating variations of (3.1) and (3.2), multiplying them by $\boldsymbol{\chi}$ and $\boldsymbol{\psi}$, respectively, and integrating, we may eliminate $\delta\boldsymbol{Y}$ and $\delta\boldsymbol{Z}$, and derive the following equation for sensitivity operators (in matrix notation)

$$\begin{aligned}
&\int\limits_{\beta}^{1}\Big(\boldsymbol{\chi}^{\top}\frac{\partial \boldsymbol{G}}{\partial h}+\boldsymbol{\psi}^{\top}\frac{\partial \mathbf{A}}{\partial h}\boldsymbol{Z}\Big)\delta h\;dx+\delta P\int\limits_{\beta}^{1}\Big(\boldsymbol{\chi}^{\top}\frac{\partial \boldsymbol{G}}{\partial P}+\boldsymbol{\psi}^{\top}\frac{\partial \mathbf{A}}{\partial P}\boldsymbol{Z}\Big)\;dx+\\
&+\delta\omega\int\limits_{\beta}^{1}\Big(\boldsymbol{\psi}^{\top}\frac{\partial \mathbf{A}}{\partial \omega}\boldsymbol{Z}\Big)\;dx=0
\end{aligned} \tag{3.6}$$

For example, in a particular case of a prescribed frequency of vibration, we obtain

$$\delta P=\int\limits_{\beta}^{1} g(x)\delta h\;dx \tag{3.7}$$

where

$$g(x)=-\frac{\boldsymbol{\chi}^{\top}\frac{\partial \boldsymbol{G}}{\partial h}+\boldsymbol{\psi}^{\top}\frac{\partial \mathbf{A}}{\partial h}\boldsymbol{Z}}{\int\limits_{\beta}^{1}\Big(\boldsymbol{\chi}^{\top}\frac{\partial \boldsymbol{G}}{\partial P}+\boldsymbol{\psi}^{\top}\frac{\partial \mathbf{A}}{\partial P}\boldsymbol{Z}\Big)\;dx} \tag{3.8}$$

If the volume of the plate is constant and the plate thickness is normalized according to formula (2.1), the Pontryagin maximum principle is equivalent to the sensitivity analysis method.

In order to determine the optimal plate thickness distribution, the Pontryagin maximum principle and an iterative procedure have been used. Starting from a uniform plate, the improved shapes have been calculated from the formula (cf. Biess *et al.*, 1980)

$$h_{n+1}=h_n+\epsilon\frac{\partial H}{\partial h}\Big|_{h_n} \tag{3.9}$$

where H is Hamiltonian (3.3) connected with state (3.1), (3.2) and appropriate adjoint equations (3.4), ϵ is a small parameter, n – iteration number. It is seen that

$$\frac{\partial H}{\partial h}=g(x)+\Lambda x \tag{3.10}$$

where Λ is a constant to be determined by constant volume condition (2.1), and that the same formula may be used for optimization under either constant loading or constant frequency constraints.

4. Equations of state

4.1. Equations of the membrane state

The basic equations of the membrane and vibration states of thin annular plates can be evaluated on the basis of the monograph by Ogibalov and Gribanov (1968).

In a basic pre-critical state, it evokes in-plane radially distributed internal compressive forces and displacements. They are determined by the following boundary value problem written in a dimensionless form

$$\begin{aligned} u' &= -\frac{\nu}{x}u + \frac{1-\nu^2}{ehx}n - (1+\nu)t \qquad && n_r = \frac{n}{x} \\ n' &= \frac{eh}{x}u + \frac{\nu}{x}n + eht && n_\theta = n' \end{aligned} \tag{4.1}$$

and

$$\alpha_1 u(\beta) + \alpha_2 n(\beta) = 0 \qquad \alpha_3 u(1) + \alpha_4 n(1) = 0 \tag{4.2}$$

We confine our consideration to plates rigidly clamped at the inner and outer edges, i.e. we assume: $\alpha_2 = \alpha_4 = 0$.

The following dimensionless variables, parameters and functions have been introduced:

— independent space variable and internal-to-external radii ratio

$$x = \frac{\overline{r}}{\overline{a}} \qquad \beta = \frac{\overline{b}}{\overline{a}} \tag{4.3}$$

— temperature distribution

$$t(x) = \frac{\overline{T}(x)}{\overline{T}_0} \tag{4.4}$$

where, in fact, the dimensional value $\overline{T}(x)$ denotes the increment of temperature distribution over its value in the stressless state, $\overline{T}_0$ denotes the reference increment of temperature,

— variable thickness and Young's modulus distributions

$$h(x) = \frac{\overline{h}}{\overline{h}_0} \qquad e[x, \overline{T}(x)] = \frac{\overline{E}[x, \overline{T}(x)]}{\overline{E}_0} \tag{4.5}$$

where some possible dependences of the Young modulus on the independent variable x and temperature $\overline{T}$ have been assumed,

— temperature loading parameter, reference plate rigidity and slenderness parameter

$$
\begin{gathered}
P = \frac{\widetilde{\alpha}}{\alpha}\overline{T}_0 \qquad\qquad \overline{D}_0 = \frac{\overline{E}_0\overline{h}_0^3}{12(1-\nu^2)} \\
\alpha = \frac{\overline{D}_0}{\overline{E}_0\overline{h}_0\overline{a}^2} = \frac{1}{12(1-\nu^2)}\Big(\frac{\overline{h}_0}{\overline{a}}\Big)^2
\end{gathered}
\tag{4.6}
$$

where ν, $\widetilde{\alpha}$, $\overline{E}_0$, $\overline{h}_0$, $\overline{T}_0$ denote Poisson's coefficient, coefficient of thermal expansion, reference Young's modulus, reference plate thickness and increment of temperature, respectively,
— displacement and compressive force

$$
\overline{u} = -P\alpha\overline{a}u(x) \qquad\qquad \overline{N} = -P\frac{\overline{D}_0}{\overline{a}}n(x)
\tag{4.7}
$$

The coefficients $\alpha_1,\dots,\alpha_4$ are certain constants.

4.2. Equations of the vibration state

It can be assumed that as a result of vibration (or buckling), the stress and strain components of the basic membrane state are subject to small variations. In contradistinction to the membrane state, the deflection and all internal forces in the vibration state are not circulary symmetric. In general they depend on the radial and angular independent variables. The well-known equation of small deflection superimposed on the membrane state of the plate may be written in the form

$$
\begin{gathered}
\frac{\partial^2(\overline{r}\overline{M}_r)}{\partial\overline{r}^2} + \frac{2}{\overline{r}}\frac{\partial^2(\overline{r}\overline{M}_{r\theta})}{\partial\overline{r}\partial\theta} + \frac{1}{\overline{r}}\frac{\partial^2\overline{M}_\theta}{\partial\theta^2} - \frac{\partial\overline{M}_\theta}{\partial\overline{r}} + \overline{r}\overline{N}_r\frac{\partial^2\overline{w}}{\partial\overline{r}^2} + \\
+\overline{N}_\theta\Big(\frac{1}{\overline{r}}\frac{\partial^2\overline{w}}{\partial\theta^2} + \frac{\partial\overline{w}}{\partial\overline{r}}\Big) - \overline{\rho}\overline{r}\overline{h}\frac{\partial^2\overline{w}}{\partial\overline{t}^2} = 0
\end{gathered}
\tag{4.8}
$$

where $\overline{w} = \overline{w}(\overline{r},\theta,\overline{t})$ is the deflection of the plate. The increments of internal forces (superposed on zero initial values) are expressed as follows

$$
\begin{aligned}
\overline{M}_r &= -\overline{D}_0 eh^3\Big[\frac{\partial^2\overline{w}}{\partial\overline{r}^2} + \nu\Big(\frac{1}{\overline{r}}\frac{\partial\overline{w}}{\partial\overline{r}} + \frac{1}{\overline{r}^2}\frac{\partial^2\overline{w}}{\partial\theta^2}\Big)\Big] \\
\overline{M}_\theta &= -\overline{D}_0 eh^3\Big[\nu\frac{\partial^2\overline{w}}{\partial\overline{r}^2} + \Big(\frac{1}{\overline{r}}\frac{\partial\overline{w}}{\partial\overline{r}} + \frac{1}{\overline{r}^2}\frac{\partial^2\overline{w}}{\partial\theta^2}\Big)\Big] \\
\overline{M}_{r\theta} &= -\overline{D}_0 eh^3(1-\nu)\frac{\partial}{\partial\overline{r}}\Big(\frac{1}{\overline{r}}\frac{\partial\overline{w}}{\partial\theta}\Big)
\end{aligned}
\tag{4.9}
$$

Now, we introduce new dimensionless variables and parameters:
— independent time variable $t = \overline{t}/\overline{t}_0$, where the dimensional constant parameter $\overline{t}_0$ may be treated as a unit of time

$$\overline{t}_0 = \sqrt{\frac{\overline{\rho}_0\overline{a}^4}{\overline{D}_0}} = \sqrt{\frac{\overline{\rho}_0\overline{a}^2}{\alpha\overline{E}_0}} \tag{4.10}$$

— frequency of vibration: $\omega = \overline{\omega}\overline{t}_0$,
— plate deflection and internal forces

$$\widetilde{w} = \frac{\overline{w}}{\overline{a}} \qquad M_j = \frac{\overline{a}\overline{M}_j}{\overline{D}_0} \qquad \text{for:} \quad j = r,\theta,r\theta \tag{4.11}$$

— mass density distribution: $\rho(x) = \overline{\rho}/\overline{\rho}_0$.

Next, we separate the functions of independent variables and we use the substitutions suggested by Grinev and Filippov (1977)

$$\begin{aligned}
&\widetilde{w}(x,\theta,t) = w(x)\mathrm{e}^{\mathrm{i}\omega t}\cos(m\theta) && M_r(x,\theta,t) = \widetilde{M}_r(x)\mathrm{e}^{\mathrm{i}\omega t}\cos(m\theta)\\
&M_\theta(x,\theta,t) = \widetilde{M}_\theta(x)\mathrm{e}^{\mathrm{i}\omega t}\cos(m\theta) && M_{r\theta}(x,\theta,t) = \widetilde{M}_{r\theta}(x)\mathrm{e}^{\mathrm{i}\omega t}\sin(m\theta)\\
&\widetilde{\widetilde{M}}_r(x) = \widetilde{M}_r(x) + \frac{1}{2}N_r(x)w(x) && \widetilde{\widetilde{M}}_\theta(x) = \widetilde{M}_\theta(x) + \frac{1}{2}N_\theta(x)w(x)\\
&\widetilde{\widetilde{M}}_{r\theta}(x) = \widetilde{M}_{r\theta}(x) && \varphi = \frac{dw}{dx} = w'\\
&M = x\widetilde{\widetilde{M}}_r && Q = M' + 2m\widetilde{\widetilde{M}}_{r\theta} - \widetilde{\widetilde{M}}_\theta\\
&N = xN_r = -Pn(x)
\end{aligned} \tag{4.12}$$

Therefore, equation (4.8) can be transformed into a set of four ordinary differential equations in a non-dimensional form

$$\begin{aligned}
&w' = \varphi \qquad\qquad \varphi' = \Big(\frac{\nu m^2}{x^2} - \frac{Pn}{2xD}\Big)w - \frac{\nu}{x}\varphi - \frac{1}{xD}M\\
&M' = \Big[(1-\nu)(3+\nu)\frac{m^2D}{x^2} - \frac{1}{2}PS\Big(\frac{u}{x} + t\Big)\Big]w +\\
&\qquad -(1-\nu)(1+\nu+2m^2)\frac{D}{x}\varphi + \frac{\nu}{x}M + Q\\
&Q' = \Big[(1-\nu)(2+\nu m^2+m^2)\frac{m^2D}{x^3} - Pm^2\frac{S}{x}\Big(\frac{u}{x}+t\Big) - \frac{P^2n^2}{4xD} - \omega^2\rho xh\Big]w +\\
&\qquad -\Big[(1-\nu)(3+\nu)\frac{m^2D}{x^2} - \frac{1}{2}PS\Big(\frac{u}{x}+t\Big)\Big]\varphi + \Big(\frac{\nu m^2}{x^2} - \frac{Pn}{2xD}\Big)M
\end{aligned} \tag{4.13}$$

where: $D = eh^3$, $S = eh$.

To equations (4.13) appropriate boundary conditions should be added. In this paper, we assume that the plate is rigidly clamped at the inner and outer edges

$$\begin{aligned} &w(\beta)=0 && \varphi(\beta)=0\\ &w(1)=0 && \varphi(1)=0 \end{aligned} \tag{4.14}$$

Of course, a variety of boundary conditions might be considered, as in the paper by Krużelecki and Smaś (2006).

Boundary value problems (4.1), (4.2) and (4.13), (4.14) consist of the so-called state equations.

4.3. Adjoint equations of the vibration state

Since the type of loading by thermal stress is conservative, the adjoint boundary value problem of the vibration state is strictly the same as state boundary value problem (4.13), (4.14). It can be shown by means of the following substitutions to Eqs (3.4)

$$\begin{aligned} &\psi_1=k\widehat{Q} && \psi_2=-k\widehat{M}\\ &\psi_3=k\widehat{\varphi} && \psi_4=-k\widehat{w} \end{aligned} \tag{4.15}$$

where k is an arbitrary constant. Therefore, the state variables $(\widehat{w},\widehat{\varphi},\widehat{M},\widehat{Q})$ can be identified with the adjoint state variables, and we can conclude that boundary value problem (4.13), (4.14) is self-adjoint.

4.4. Adjoint equations of the membrane state

Substituting new adjoint membrane state variables

$$\chi_1=k_1\widehat{n} \qquad\qquad \chi_2=-k_1\widehat{u} \tag{4.16}$$

the system of adjoint differential equations of the membrane state can be written in the form

$$\begin{aligned} \widehat{u}'&=-\frac{\nu}{x}\widehat{u}+\frac{1-\nu^2}{xeh}\widehat{n}+\frac{P}{2xeh^3}(2Mw+Pnw^2)\\ \widehat{n}'&=\frac{eh}{x}\widehat{u}+\frac{\nu}{x}\widehat{n}+Peh\Big(\frac{1}{x}w\varphi-\frac{m^2}{x^2}w^2\Big) \end{aligned} \tag{4.17}$$

Here, the appropriate adjoint boundary conditions are the same as for the state functions

$$\widehat{u}(\beta)=0 \qquad\qquad \widehat{u}(1)=0 \tag{4.18}$$

5. Numerical calculations and results

5.1. Numerical calculations

Numerical calculations can be performed for some types of temperature distributions, suggested by Ogibalov and Gribanov (1968), for example

$$t(x) = \frac{1-x^2}{1-\beta^2} \qquad \text{or} \qquad t(x) = 1 - \Big(\frac{x-\beta}{1-\beta}\Big)^n \tag{5.1}$$

However, we confined our calculations to the first formula and for boundary conditions (4.2) and (4.14). In all calculations β was set equal to 0.2 and Poisson's ratio ν was assumed to be 0.25. The reference density was assumed to be equal to the plate density and, as a result, $\rho \equiv 1$. All differential equations were solved by the Runge-Kutta-Gill integration method of the fourth order, using the transfer matrix method (cf. Gajewski, 2002). The gradient function was calculated from the formula

$$\begin{aligned}\frac{\partial H}{\partial h} &= \Big[\Lambda x + \rho x\omega^2 w^2 + e\Big(\frac{u}{x} + t\Big)\Big(P\frac{m^2}{x}w^2 - Pw\varphi - \widehat{u}\Big)\Big] + \\ &-h^2\Big\{3(1-\nu)e\Big[(2+\nu m^2+m^2)\frac{m^2}{x^3}w^2 + (1+\nu+2m^2)\frac{1}{x}\varphi^2 + \\ &-2(3+\nu)\frac{m^2}{x^2}w\varphi\Big]\Big\} - \frac{1}{h^2}\Big[\frac{(1-\nu^2)}{ex}n\widehat{n}\Big] - \frac{1}{h^4}\frac{3}{ex}\Big(M + \frac{1}{2}Pnw\Big)^2\end{aligned} \tag{5.2}$$

which can be used both under constant loading and constant frequency constraints.

Moreover, we have imposed additional geometrical constraints on the plate thickness

$$h_{11} \leqslant h(x) \leqslant h_{22} \tag{5.3}$$

where: $h_{11} = 0.5$ and $h_{22} = 3.0$.

5.2. Results

5.2.1. A plate of constant thickness

At first, the dependence of the compressive force parameter (temperature) on the frequency of vibration is presented in Fig. 2. In the picture, the first and second vibration frequency for $m = 0,\dots,4$ in relation to thermal loading are plotted.

From the first picture in Fig. 2, one can conclude that for $P \lesssim 200$ the starting point to the optimization procedure should be a plate of constant

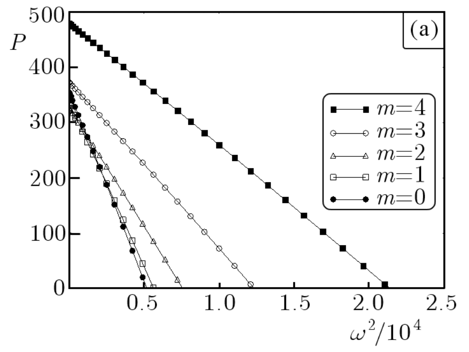

Fig. 2. Thermal loading versus: (a) the first frequency and (b) second frequency of vibration

thickness with $m = 0$. However, for greater values of P we must start with $m = 1$ or even $m = 2$. During the iteration process, values of circumferential waves m can undergo changes.

5.2.2. *The optimization with respect to frequency of vibration under constant loading*

As the first example of the optimization procedure, we present in Fig. 3 plate shapes obtained in consecutive iterations for a very small value of temperature loading. In fact, it is an optimization with respect to the vibration frequency only. It is seen in the Fig. 4 that the convergence of the iteration process is regular and very quick. The frequency of vibration increases from $\omega_{prism} \approx 72$ for the plate of constant thickness up to $\omega_{opt} \approx 95$ for the optimal plate. The optimization has been performed for $m = 0$.

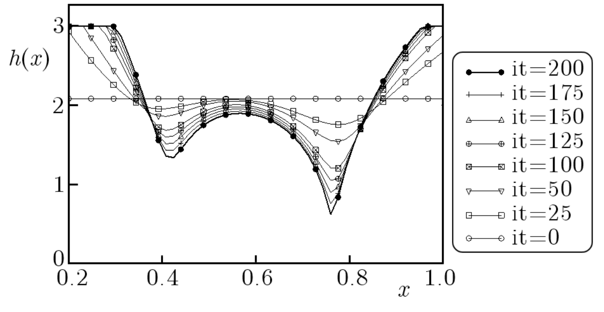

Fig. 3. Plate thickness in consecutive iterations ($P = 1$, $h_{11} = 0.5$, $h_{22} = 3.0$, $\omega \to \max$, $m = 0$)

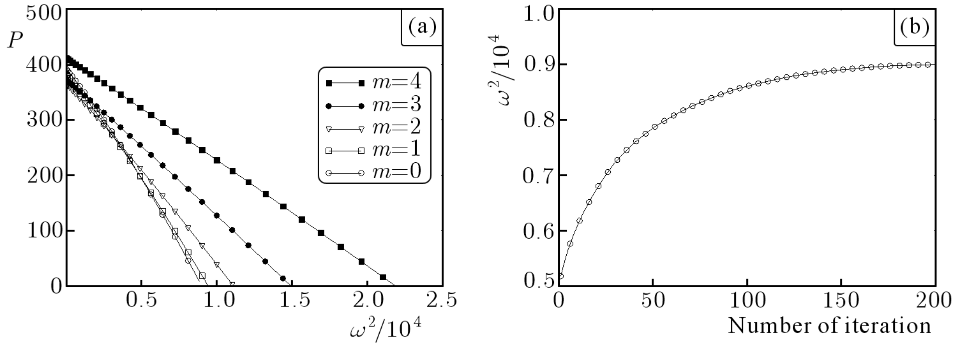

Fig. 4. (a) Characteristic curves for the optimal plate $(P = 1,\ h_{11} = 0.5,\ h_{22} = 3.0,$ $\omega \to \max)$ and (b) convergence of the optimization process $(P = 1,\ \omega \to \max)$

5.2.3. The optimization with respect to thermal loading under constant frequency constraint

As the second example, we present in Fig. 5 plate shapes obtained in consecutive iterations for a very small value of the vibration frequency. In fact, it is an optimization with respect to thermal loading only (under stability constraints).

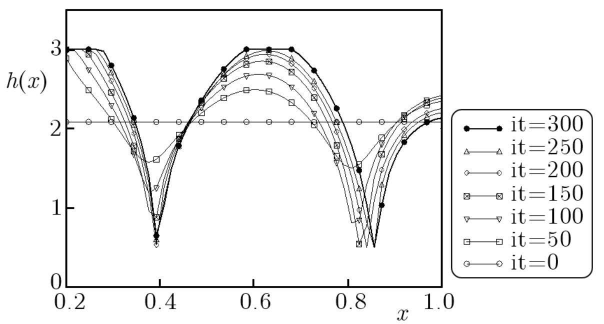

Fig. 5. Plate thickness in consecutive iterations $(P \to \max,\ P_{opt} = 532,\ \omega = 10,$ $\varepsilon = 0.05)$

It is seen in Fig. 6 that the convergence of the iteration process is not so regular as in the previous example. The buckling thermal loading increases from $P_{prism} \approx 326$ for the plate of constant thickness to $P_{opt} \approx 532$ for the optimal plate. The optimization had to be performed for $m = 2$. Moreover, the optimal shape is practically a three-modal solution, for which: $P_{opt}(m = 0) \approx 532.5$, $P_{opt}(m = 1) \approx 531.9$, $P_{opt}(m = 2) \approx 534.0$.

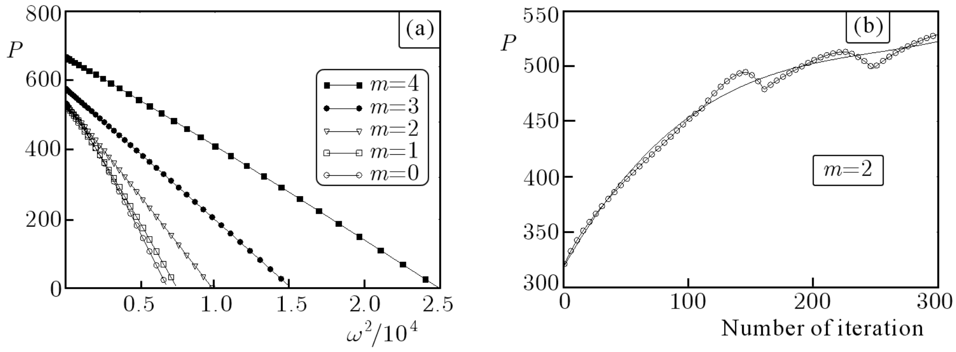

Fig. 6. (a) Characteristic curves for the optimal plate $(P_{opt} = 532, \omega = 10)$ and (b) convergence of the optimization procedure $(P \to \max, P_{opt} = 532, \omega = 10)$

5.2.4. Optimal plate shapes for various thermal loading levels

The calculations similar to those presented in the previous subsections enable one to construct the final results. They are shown in Fig. 7, where the optimal plate shapes obtained for various thermal loading levels are illustrated. Of course, the optimal shape under the buckling constraint (for $\omega = 0$) is quite different from that obtained under the vibration frequency constraint (for $P = 0$).

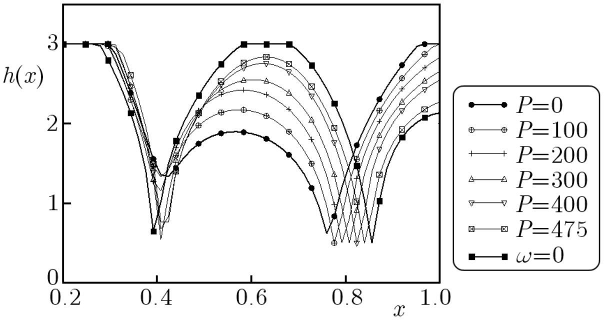

Fig. 7. Optimal plates for various thermal loading levels

5.2.5. The influence of temperature on the Young modulus

In all results presented above, the Young modulus was treated as a certain constant independent of temperature. However, it should be noted that the increase of temperature (loading parameter P) causing buckling of the plate is rather high. Therefore, the Young modulus changes its value according to the increase of temperature. This phenomenon can influence the optimal shapes of the plate. To consider this, we have fitted the experimental data presented in Fig. 8 (given by Odquist, 1966), with a polynomial of the third degree

$$\overline{E} = \overline{E}_0 e(\overline{T}) = \overline{E}_0(1 - \overline{a}\overline{T} + \overline{b}\overline{T}^2 - \overline{c}\overline{T}^3) \tag{5.4}$$

where

$$\begin{aligned} &\overline{E}_0 = 197\,\text{MPa} && \overline{a} = 3.92 \cdot 10^{-4}[^\circ\text{C}]^{-1} \\ &\overline{b} = 1.77 \cdot 10^{-6}[^\circ\text{C}]^{-2} && \overline{c} = 3.30 \cdot 10^{-9}[^\circ\text{C}]^{-3} \end{aligned} \tag{5.5}$$

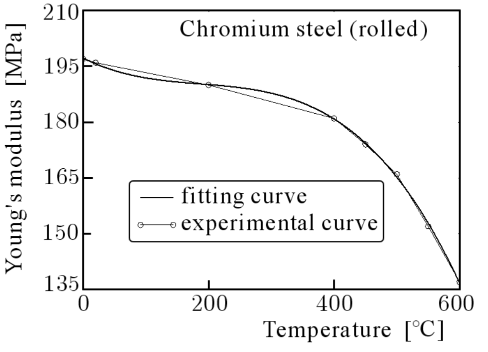

Fig. 8. Dependence of the Young modulus on teperature

As it is seen in Fig. 8., function (5.4) describes quite well the real dependence of the Young modulus on temperature. In numerical calculations, formula (5.4) is written in the dimensionless form

$$e[\overline{T}(x)] = 1 - \overline{a}[\overline{\xi}Pt(x)] + \overline{b}[\overline{\xi}Pt(x)]^2 - \overline{c}[\overline{\xi}Pt(x)]^3 \tag{5.6}$$

in which the dimensional parameter $\overline{\xi}$ has been introduced

$$\overline{\xi} = \frac{\alpha}{\widetilde{\alpha}} \qquad [\overline{\xi}] = [^\circ\text{C}] \qquad \overline{\xi} \approx (1 \div 20)[^\circ\text{C}] \tag{5.7}$$

To illustrate the influence of the relationship between the Young modulus and temperature on the optimal plate shape, we performed calculations for several values of the parameter $\overline{\xi}$ for a constant thermal loading $P = 300$ and $m = 1$. Moreover, in this case, the membrane state without any stress is assumed at the temperature 0°C.

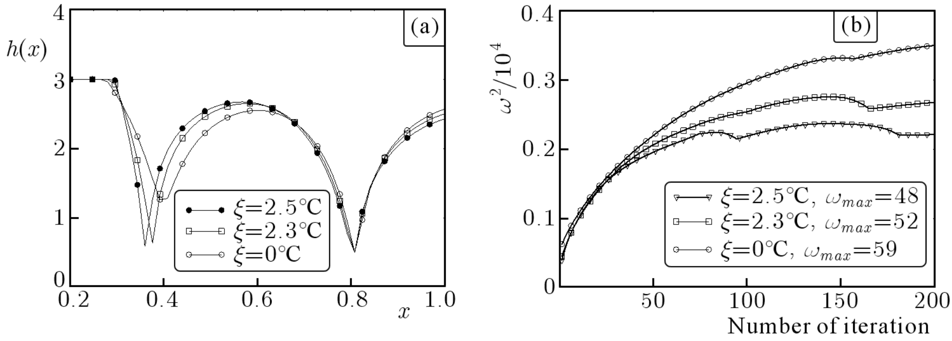

Fig. 9. (a) Optimal plate shapes and (b) convergence of the optimization procudure for various values of the coefficient $\overline{\xi}$ ($P = 300$, $h_{11} = 0.5$, $h_{22} = 3.0$, $\omega \to \max$, $m = 1$)

6. Conclusions

In the paper, a significant difference between the optimal plate shapes obtained under buckling or vibration constraints has been demonstrated. It should be noted that for some cases of boundary conditions the optimization with respect to the lowest frequency of vibration (or the lowest buckling thermal loading) may result in the lowering of a higher-order eigenvalue below the first one. Then the result of a unimodal optimal design (i.e. with respect to single eigenvalue) is false, and a multimodal optimal design should be employed. Additionally, it has been shown that the dependence of the Young modulus on temperature can have great influence on the optimal shapes.

Acknowledgment

Partial support of this work under Grant 5T07A-003-24 by the State Committee for Scientific Research is gratefully acknowledged.

References

1. Biess G., Erfurth H., Zeidler G., 1980, *Optimale Prozesse und Systeme*, BSB B.G.Teubner, Leipzig

2. Frauenthal J.C., 1972, Constrained optimal design of circular plates against buckling, *J. Struct. Mech.*, **1**, 115-127

3. Gajewski A., 2001, Optimization of elastic annular plates subject to thermal stresses under buckling constraints, *"Optimization in Industry III"*, Ref. Num-

ber 06, US United Engineering Foundation, June 17-22, Ciocco-Barga, Italy (Eds.: I.C. Parmee, P. Hajela)

4. Gajewski A., 2002a, Optimization of elastic annular plates subject to thermal stresses under vibration constraints, *Proc. Vibration in Physical Systems*, XXth Jubilee Symposium, Poznań-Błażejewko, May 21-25, 2002, 150-151, Politechnika Poznańska, Poznań
5. Gajewski A., 2002b, Vibration and stability of annular plates in non-linear creep conditions, *J. Sound and Vibr.*, **249**, 3, 447-463
6. Gajewski A., Cupiał P., 1992, Optimal structural design of an annular plate compressed by non-conservative forces, *Int. J. Solids Structures*, **29**, 10, 1283-1292
7. Gajewski A., Życzkowski M., 1988, *Optimal Structural Design under Stability Constraints*, Kluwer Academic Publishers, Dordrecht
8. Grinev V.B., Filippov A.P., 1977, Optimal design of circular plates in stability problems, *Stroit. Mech. i Raschot Sooruzeniy*, **2**, 16-20 [in Russian]
9. Krużelecki J., Smaś P., 2006, Optimal annular plates with respect to their stability under thermal loadings, *Struct. Multidisc. Optim.*,**32**, 111-120
10. Mermertas V., Belek H.T., 1990, Static and dynamic stability of variable thickness annular plates, *J. Sound and Vibr.*, **141**, 435-448
11. Odqvist F.K.G., 1966, *Mathematical theory of creep and creep rupture*, Clarendon Press, Oxford
12. Ogibalov P.M., Gribanov W.F., 1968, *Thermo-stability of plates and shells*, Moscow University Press [in Russian]
13. Rzegocińska-Pełech K., Waszczyszyn Z., 1984, Numerical optimum design of elastic annular plates with respect to buckling, *Computers & Struct.*, **18**, 369-378
14. Wróblewski A., 1992, Optimal design of circular plates against creep buckling, *Eng. Opt.*, **20**, 111-128

Optymalizacja płyt pierścieniowych z uwagi na drgania przy obciążeniach termicznych

Streszczenie

W pracy badano problemy optymalizacji płyt pierścieniowych poddanych działaniu równomiernie rozłożonych obciążeń temperaturowych, z uwagi na częstość drgań.

Poszukiwano takiego rozkładu grubości płyty (kołowo symetrycznej) o stałej objętości, który prowadzi do maksymalizacji jej częstości drgań. Ograniczono się do płyty utwierdzonej na brzegu zewnętrznym i brzegu wewnętrznym oraz do jednego typu niejednorodności rozkładu temperatury. Przyjęto również nierównościowe warunki geometryczne nałożone na minimalną i maksymalną grubość płyty. Jako metodę rozwiązania zagadnienia przyjęto zasadę maksimum Pontryagina połączoną z analizą wrażliwości i metodą gradientową.

Manuscript received March 19, 2008; accepted for print May 19, 2008